

Growth of ordered C₆₀ islands on TiO₂(110)

Felix Loske, Ralf Bechstein, Jens Schütte, Frank Ostendorf, Michael Reichling and Angelika Kühnle

Fachbereich Physik, Universität Osnabrück, BarbarasträÙe 7, 49076 Osnabrück, Germany

E-mail: kuehnle@uos.de

Received 9 October 2008, in final form 23 November 2008

Published 15 January 2009

Online at stacks.iop.org/Nano/20/065606

Abstract

Non-contact atomic force microscopy is used to study C₆₀ molecules deposited on the rutile TiO₂(110) surface *in situ* at room temperature. At submonolayer coverages, molecules adsorb preferentially at substrate step edges. Upon increasing coverage, ordered islands grow from the decorated step edges onto the lower terraces. Simultaneous imaging of bridging oxygen rows of the substrate and the C₆₀ island structure reveals that the C₆₀ molecules arrange themselves in a centered rectangular superstructure, with the molecules lying centered in the troughs formed by the bridging oxygen rows. Although the TiO₂(110) surface exhibits a high density of surface defects, the observed C₆₀ islands are of high order. This indicates that the C₆₀ intermolecular interaction dominates over the molecule–substrate interactions that may cause structural perturbations on a defective surface. Slightly protruding C₆₀ strands on the islands are attributed to anti-phase boundaries due to stacking faults resulting from two islands growing together.

(Some figures in this article are in colour only in the electronic version)

1. Introduction

The adsorption of molecules onto surfaces has been studied intensively motivated by promising future applications in a wide range of fields including molecular electronics [1, 2]. Reliable molecular electronic devices operation does, however, require precise control of both, molecular structure formation and structural perfection. Thus, systems are needed that provide highly ordered as well as contaminant and defect-free layers [3, 4].

In particular, C₆₀ molecules [5] have attracted great attention as candidates for molecular electronic devices due to their intrinsic amplifier effect [6] and have been proposed for single-molecule transistor applications [7]. Furthermore, they are used in organic solar cells as strong electron acceptors [8–10]. Consequently, C₆₀ has been studied on a broad variety of different substrates, including metallic [11–13], semiconducting [14, 15] as well as insulating [16–19] surfaces. The (110) surface of rutile titanium dioxide [20–23] is one of the most intensively studied oxide surfaces and represents a prototypical system for transition metal oxides [24]. It is widely used in catalytic as well as photoelectrochemical applications [25–27].

In this work, we study the principles of adsorption of C₆₀ on rutile TiO₂(110) by non-contact atomic force microscopy (NC-AFM) under ultra-high vacuum (UHV) conditions, allowing for high-resolution imaging at the subnanometer scale. Our results reveal the formation of strikingly ordered, nearly defect-free islands with a rather regular shape. Straight lines of protruding C₆₀ molecules identified as anti-phase boundaries are found to run along two distinct lattice directions.

2. Experimental setup

Measurements were performed at room temperature with a VT-AFM 25 atomic force microscope (Omicron, Taunusstein, Germany) equipped with an easyPLL Plus phase-locked loop controller and detector (Nanosurf, Liestal, Switzerland) operated in the frequency modulation non-contact mode under UHV conditions with a base pressure better than 1×10^{-10} mbar. For NC-AFM imaging, silicon cantilevers (PPP-NCH Nanosensors, Neuchâtel, Switzerland) with resonance frequencies of about 300 kHz and typical quality factors of 30 000 were excited to oscillations with an amplitude of 10 nm. Tips were Ar⁺ ion sputtered (2 keV, 5 min)

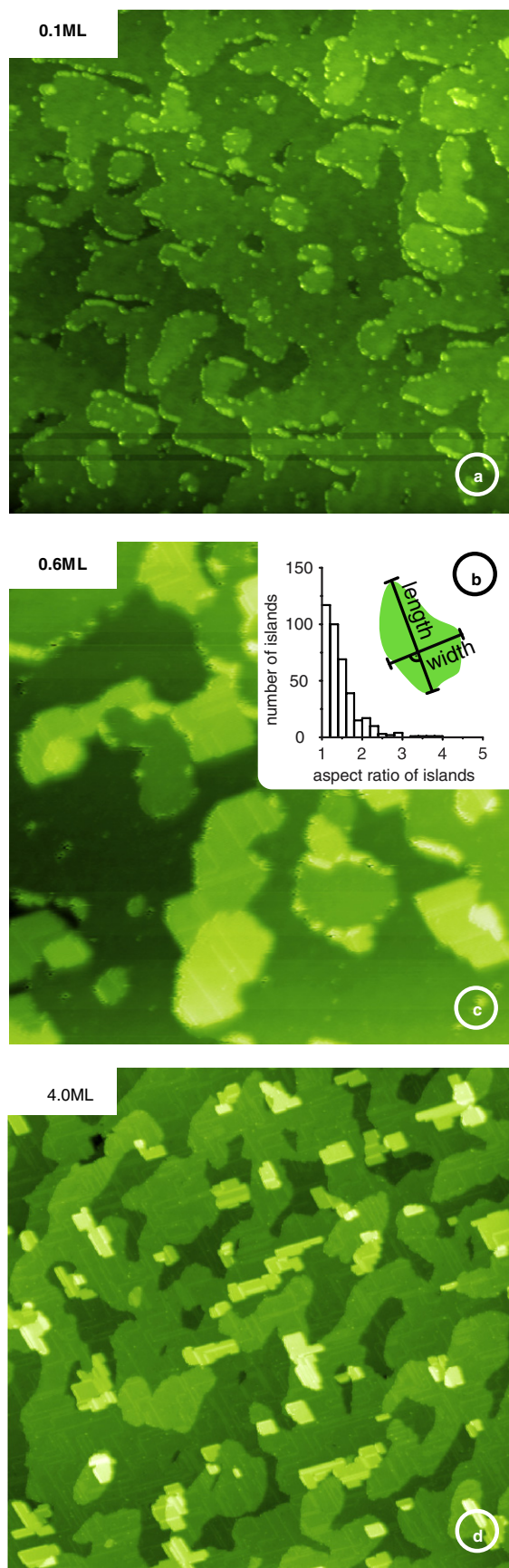


Figure 1. C₆₀ on TiO₂(110) at different coverages (*z* contrast images). (a) 0.1 ML C₆₀, 440 nm × 440 nm. (b) Histogram of the aspect ratios. (c) 0.6 ML C₆₀, 194 nm × 194 nm. (d) 4.0 ML C₆₀, 440 nm × 440 nm.

to remove contaminants. In order to minimize long-range electrostatic interactions, an appropriate bias voltage was applied to the tip. The compensating voltage was determined via Kelvin probe force spectroscopy [28]. Depending on the distance feedback loop settings, either constant frequency shift (*z* contrast) or constant height images (*df* contrast) were taken [29]. Rutile TiO₂ samples were crystals of highest available quality (MTI, Richmond, USA). The surface was cleaned by repeated cycles of Ar⁺ sputtering (1 keV) and annealing at 1100 K. The C₆₀ molecules (purity of 99.95%, MER Corporation, Tuscon, Arizona) were deposited onto the surface by thermal evaporation from a home-made Knudsen cell heated to 500 K. The substrate was at room temperature. The deposition rate of 0.12 ML min⁻¹ (1 ML equals to 0.2 C₆₀ molecules per TiO₂(110) unit cell) was estimated with a quartz crystal deposition monitor (Inficon, East Syracuse, USA).

3. Results and discussion

Upon submonolayer deposition, molecules are observed to preferentially adsorb at step edges as shown in figure 1(a). With increasing coverage, islands appear to grow from substrate step edges onto the lower terraces as seen in figure 1(c). By far the most islands are attached to a substrate step edge and only very few grow directly on terraces, the latter islands are ascribed to nucleation at defect sites. For a statistical analysis, we investigate the shape of the islands in more detail. In total 381 islands from eight different images taken at different submonolayer coverages were analyzed; and a histogram of the aspect ratios (length divided by the width for the best fitting rectangle) is depicted in figure 1(b). This histogram reflects the overall rather compact shape of the C₆₀ islands. For higher coverages, large C₆₀ islands are formed in a Stranski–Krastanov growth mode, covering the entire substrate as seen in figure 1(d).

Single C₆₀ molecules on terraces are observed rarely; some of them are seen in figure 2(a). These individual molecules are assumed to be anchored at surface defects. The density of the most prevalent surface defects, namely single and double hydroxyls originating from oxygen vacancies amounts to 4% ML for this particular sample after 19 cycles of sputtering and annealing [30]. As this density is much higher than the density of the individual C₆₀ molecules observed in our experiments, the fixed C₆₀ molecules must be anchored at other defect sites that are not yet identified. These fixed molecules are supposed to act as nucleation seeds for the growth of the few C₆₀ islands found on terraces.

In the lower part of figure 2(a) a C₆₀ island edge is shown. The bridging oxygen rows can be identified by the position of hydroxyl defects, which are known to form on the bridging oxygen rows from oxygen vacancies through water adsorption [30, 32]. In figure 2 the bright (larger negative frequency shift) rows correspond to the substrate bridging oxygen rows running along the [001] direction, since surface defects (single and double hydroxyls) appear as brighter spots on these rows (one is indicated by an arrow) [32]. In the upper half of the image, four additional features are found (dashed circles) that are much larger than typical surface defects.

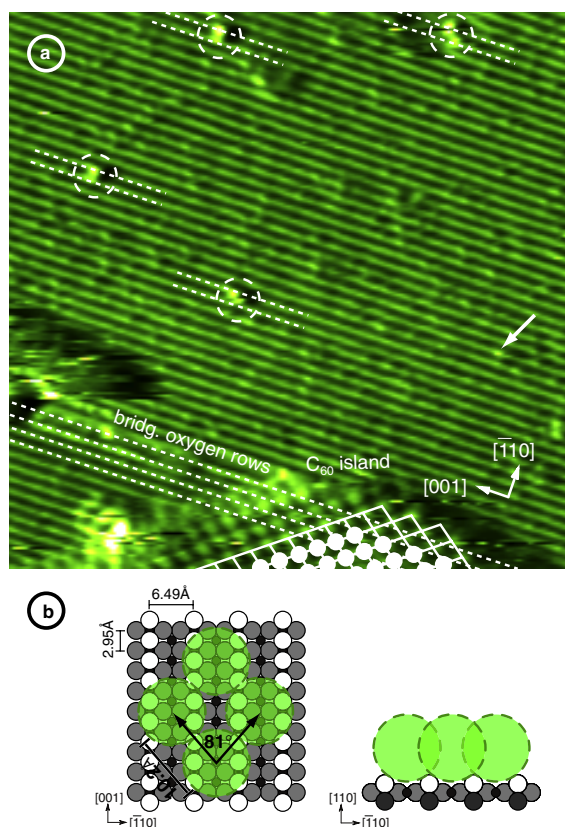


Figure 2. Single C_{60} molecules and C_{60} islands imaged on an area of $25 \text{ nm} \times 25 \text{ nm}$, df contrast. Single C_{60} molecules (dashed circles) and hydroxyl defects (one is indicated by an arrow) on a terrace (upper part) and C_{60} island attached to a step edge (lower part) are shown. Before molecule evaporation, this surface has been cleaned by 19 cycles of sputtering and annealing, the density of hydroxyl defects corresponds to 4% ML. (b) Model of the C_{60} island structure. The C_{60} molecules are sketched with their van der Waals radii ($\approx 10 \text{ \AA}$ [31]). The molecules are centered in the troughs formed by the bridging oxygen rows. The exact lattice site within the troughs, however, cannot be determined and is arbitrary in the given model.

These features are ascribed to single C_{60} molecules, adsorbed between the bridging oxygen rows (dashed lines). In the lower half of the image, a C_{60} island anchored to a substrate step edge is shown. As can be seen by comparison of C_{60} covered and uncovered areas, also within an island C_{60} molecules adsorb in the troughs formed by the bridging oxygen rows. Molecules arrange in a centered rectangular superstructure. The angle spanned by the basis vectors of the superstructure amounts to $81^\circ \pm 2^\circ$. The nearest-neighbor distance between the molecules is measured to $10.0 \text{ \AA} \pm 0.2 \text{ \AA}$, the same as in the bulk C_{60} crystal (10.0 \AA [33]). As atomic resolution is lost at C_{60} island edges, the exact adsorption site in [001] direction cannot be determined. The measured dimensions do, however, agree with a $c(5 \times 2)$ superstructure within the error of our length measurements. We could not resolve any structure within the molecules, which might be due to the fact that the molecules possess sufficient thermal energy for rotating around their center as in bulk C_{60} [34].

These findings suggest that the assembly at room temperature is driven by the C_{60} intermolecular interaction,

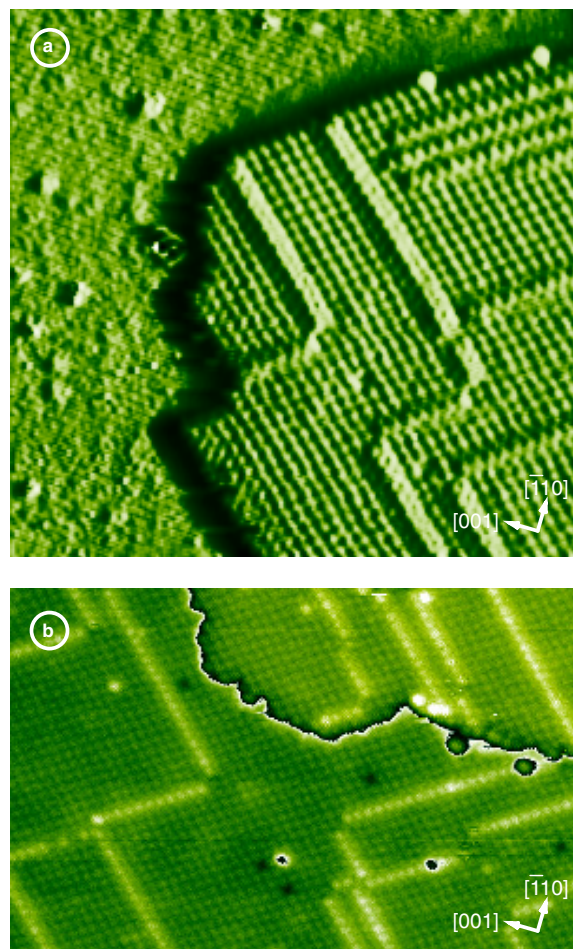


Figure 3. z contrast images showing domain boundaries running across C_{60} islands. (a) 0.5 ML C_{60} , $42 \text{ nm} \times 40 \text{ nm}$. To enhance the contrast, the derivative of the z channel is shown. (b) 4.0 ML C_{60} , $53 \text{ nm} \times 27 \text{ nm}$. To enhance the contrast, a repeating color scale is used.

while the substrate is templating the molecules in between the bridging oxygen rows. Moreover, the C_{60} molecules seem to possess sufficient kinetic energy to diffuse on the surface. Consequently, the island growth requires nucleation sites such as step edges or pinned molecules.

A recent study using scanning tunneling microscopy on the $\text{TiO}_2(110) 1 \times 2$ cross-link reconstructed surface has revealed a similar behavior [19]. In this study, the C_{60} molecules have been observed to anchor at the cross-link sites and to grow along the [001] direction in the troughs. The observed C_{60} adsorption position on top of the Ti rows agrees with the findings in our study. It has been argued that C_{60} anchors to the undercoordinated Ti cations while the intermolecular interaction is governed by van der Waals interaction, in good agreement what we observe on the unreconstructed surface.

An impression of the regular order and shape of the islands is shown in figure 3(a), exhibiting an island after 0.5 ML deposition. A closer inspection of the C_{60} islands reveals straight lines of bright appearing C_{60} molecules, running parallel to the basis vectors of the superstructure along the $[\bar{2}25]$ and $[\bar{2}\bar{2}5]$ directions. These lines are also observed at

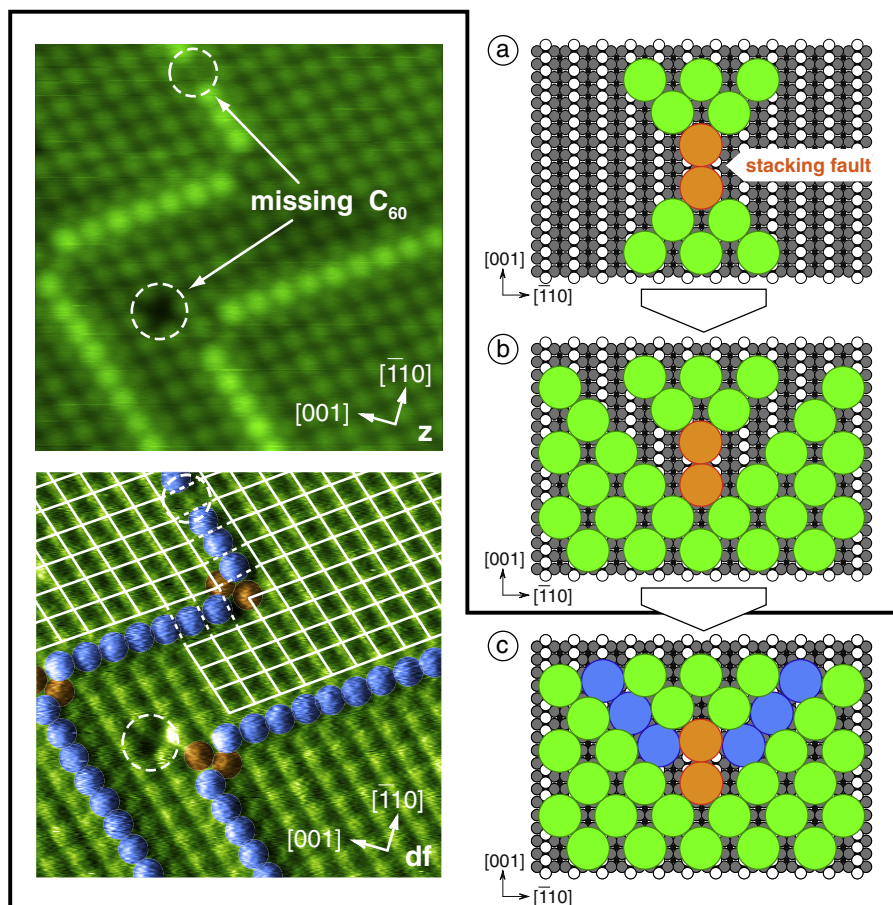


Figure 4. Anti-phase boundaries due to stacking faults. Right panel: (a) C_{60} molecules causing a stacking fault are colored red. (b) During island growth a gap is created between the islands growing together, which cannot be occupied by C_{60} molecules. (c) C_{60} molecules adsorb on this gap (colored blue), resulting in protruding rows of single C_{60} strands, running in the $[2\bar{2}5]$ and $[\bar{2}25]$ directions. Left panel: C_{60} island, showing domain boundaries and defects in z (upper image) and df (lower image) channel; $14\text{ nm} \times 14\text{ nm}$. Two defects are marked: a missing C_{60} molecule within a protruding strand and a single missing molecule within a C_{60} island.

higher coverages, as shown in figure 3(b), representing the molecular ordering after 4.0 ML deposition. The straight lines consist of single strands of molecules slightly protruding from the C_{60} islands. Since these lines do not occur periodically in any way, it can be excluded that they are due to a lattice mismatch between the C_{60} superstructure and the substrate unit cell. Neither underlying surface defects such as oxygen vacancies or hydroxyls can be the reason, considering that the defect density is much higher than the number of protruding lines. A plausible explanation for these lines of protruding molecules are, however, anti-phase boundaries originating from stacking faults.

We propose that such domain boundaries originate from two islands growing together. If two molecules are in close contact within a trough, an anti-phase boundary is created as illustrated by the red-colored C_{60} molecules in figure 4(a). This stacking fault results in a gap between the two islands that cannot be occupied by C_{60} molecules due to the limited space (figure 4(b)). However, molecules adsorb on top of these boundaries between two coalescing islands (colored blue in figure 4(c)). More precisely, these molecules lie on the imaginary center of the area spanned by four molecules (two

of each island), which corresponds to a maximization of the number of nearest-neighbors.

Considering the size of the C_{60} islands and the typical density of surface hydroxyl defects, which is in the range of 2%–6% ML in our experiments (note: 1 ML of defects equals to one defect per $\text{TiO}_2(110)$ unit cell) [30], surface defects do exist underneath the C_{60} islands. On the C_{60} islands, however, structural imperfections other than domain boundaries are observed only very rarely. These C_{60} island defects are single missing molecules as those shown in figure 4. The number of C_{60} island defects is by far too small to account for the number of underlying substrate defects, indicating that surface defects do not perturb the island growth. Our results, therefore, demonstrate that defect-free C_{60} layers can be prepared on a surface with an initially high density of surface defects.

4. Summary and conclusion

In summary, we find that C_{60} molecules are mobile on the rutile $\text{TiO}_2(110)$ surface at room temperature. Single C_{60} molecules diffuse over the surface and require nucleation sites for island growth, such as step edges or substrate defects. Molecules

adsorb in the troughs formed by the bridging oxygen rows of the substrate. The C₆₀ island superstructure is found to be centered rectangular with an angle of $81^\circ \pm 2^\circ$ spanned by the basis vectors, in agreement with a $c(5 \times 2)$ superstructure. Although the underlying TiO₂(110) surface is known to exhibit a high density of defects, the C₆₀ islands are almost free of defects and have a regular, compact shape. The system introduced here offers a great potential for the deposition of highly ordered monomolecular layers of C₆₀ on an insulating substrate. Deposition in a nano-stencil system [35] would facilitate the fabrication of shaped nano-pads for molecular electronic applications e.g. as molecular contacts.

Acknowledgments

Stimulating discussions with Joachim Wollschläger are gratefully acknowledged. This work has been supported by the German Research Foundation (DFG) through the Emmy Noether-program and the integrated project PicoInside of the European Union.

References

- [1] Joachim C, Gimzewski J K and Aviram A 2000 *Nature* **408** 541
- [2] Aviram A and Ratner M A 1974 *Chem. Phys. Lett.* **29** 277
- [3] Tang C W 1986 *Appl. Phys. Lett.* **48** 183
- [4] Forrest S R 2004 *Nature* **428** 911
- [5] Kroto H W, Heath J R, O'Brien S C, Curl R F and Smalley R E 1985 *Nature* **318** 162
- [6] Joachim C and Gimzewski J K 1997 *Chem. Phys. Lett.* **265** 353
- [7] Joachim C, Gimzewski J K and Tang H 1998 *Phys. Rev. B* **58** 16407
- [8] Miller B, Rosamilia J M, Dabbagh G, Tycko R, Haddon R C, Muller A J, Wilson W, Murphy D W and Hebard A F 1991 *J. Am. Chem. Soc.* **113** 6291
- [9] Sariciftci N S, Smilowitz L, Heeger A J and Wudl F 1992 *Science* **258** 1474
- [10] Yu G, Gao J, Hummelen J C, Wudl F and Heeger A J 1995 *Science* **270** 1789
- [11] Altman E I and Colton R J 1993 *Phys. Rev. B* **48** 18244 LP
- [12] Mativetsky J M, Burke S A, Hoffmann R, Sun Y and Grütter P 2004 *Nanotechnology* **15** 40
- [13] Hashizume T *et al* 1993 *Phys. Rev. Lett.* **71** 2959
- [14] Suto S, Sakamoto K, Wakita T, Harada M and Kasuya A 1998 *Surf. Sci.* **402–404** 523
- [15] Kobayashi K, Yamada H, Horiuchi T and Matsushige K 1999 *Appl. Surf. Sci.* **140** 281
- [16] Burke S A, Mativetsky J M, Hoffmann R and Grütter P 2005 *Phys. Rev. Lett.* **94** 096102
- [17] Burke S A, Mativetsky J M, Fostner S and Grütter P 2007 *Phys. Rev. B* **76** 035419
- [18] Murray P W, Gimzewski J K, Schlittler R R and Thornton G 1996 *Surf. Sci.* **367** L79
- [19] Fukui K and Sakai M 2006 *J. Phys. Chem. B* **110** 21118
- [20] Fukui K-I, Onishi H and Iwasawa Y 1997 *Phys. Rev. Lett.* **79** 4202
- [21] Pang C L, Raza H, Haycock S A and Thornton G 2000 *Appl. Surf. Sci.* **157** 233
- [22] Onishi H, Sasahara A, Uetsuka H and Ishibashi T 2002 *Appl. Surf. Sci.* **188** 257
- [23] Lauritsen J V, Foster A S, Olesen G H, Christensen M C, Kühnle A, Helveg S, Rostrup-Nielsen J R, Clausen B S, Reichling M and Besenbacher F 2006 *Nanotechnology* **17** 3436
- [24] Diebold U 2003 *Surf. Sci. Rep.* **48** 53
- [25] Fujishima A and Honda K 1972 *Nature* **238** 37
- [26] Grätzel M 2001 *Nature* **414** 338
- [27] Linsebigler A L, Lu G and Yates J T J 1995 *Chem. Rev.* **95** 735
- [28] Zerweck U, Loppacher C, Otto T, Grafström S and Eng L M 2005 *Phys. Rev. B* **71** 125424
- [29] Gritschneider S, Namai Y, Iwasawa Y and Reichling M 2005 *Nanotechnology* **16** S41
- [30] Wendt S *et al* 2005 *Surf. Sci.* **598** 226
- [31] Krättschmer W, Lamb L D, Fostiropoulos K and Huffman D R 1990 *Nature* **347** 354
- [32] Enevoldsen G H, Foster A S, Christensen M C, Lauritsen J V and Besenbacher F 2007 *Phys. Rev. B* **76** 205415
- [33] Heiney P A, Fischer J E, McGhie A R, Romanow W J, Denenstien A M, McCauley J P Jr, Smith A B and Cox D E 1991 *Phys. Rev. Lett.* **66** 2911
- [34] Yannoni C S, Johnson R D, Meijer G, Bethune D S and Salem J R 1991 *J. Phys. Chem.* **95** 9
- [35] Zahl P, Bammerlin M, Meyer G and Schlittler R R 2005 *Rev. Sci. Instrum.* **76** 023707